Transitions in Thermal Circulations in the Atmospheric Boundary Layer

John R. Taylor

School of Physical, Environmental and Mathematical Sciences
UNSW Canberra, Canberra, Australian Capital Territory, 2600, Australia

Abstract

Unsteady, thermally-driven mesoscale circulation in the atmospheric boundary layer was simulated in a water tank model. The circulation was forced by applying a heat flux at the bottom of one half of an experimental tank. The heat flux could be rapidly switched between heating and cooling while the other, neutral, half of the tank had a constant temperature lower boundary that was maintained approximately midway between the maximum and minimum temperatures for the forced half of the tank. Vertical slices of the water velocities in both sections of the tank were acquired using particle image velocimetry, while horizontal traverses of fast response thermistors were used to measure temperatures.

On the heated side of the tank convective plumes initially developed uniformly along the tank, but a circulation soon set up at the boundary between the heated and neutral regions. The outflow into the neutral region was a simple gravity current, travelling along the upper boundary. In contrast, water from the neutral side penetrated much more slowly over the heated boundary as the convective plumes mixed the horizontal momentum of the flow vertically. The net result was a highly asymmetric circulation with the internal Froude number of the cool inflow over the heated boundary being much smaller than would be expected from gravity current dynamics. When the forcing was switched, the stabilizing buoyancy flux rapidly shut down the convection, and the density front over the heated side rapidly collapsed.

Introduction

Thermally-driven circulations are common mesoscale features in the atmospheric boundary layer. The most well-known of these is the sea/land breeze cycle, driven by the contrast in the response of land and ocean surfaces to the diurnal radiation cycle. These flows are unsteady, and, in the atmospheric boundary layer their dynamics can change over timescales of a few hours. As an example, early evening easterly wind changes are often observed in Canberra during the summer [1, 10]. Locally these wind changes are generally referred to as sea-breeezes, as the direction of the following wind and higher dew points in the air masses behind the change, are consistent with a maritime origin for the intruding air mass. On the other hand, in both [1] and [10] it is suggested that they are linked with more complex phenomena than a simple land/sea temperature contrast. Examples of this "sea-breeze" can be observed as far inland as as Wagga Wagga Airport, approximately 300 km from the coast where they arrive at around midnight. In [1] apparently similar flows in other regions in Australia are described; these propagate equally impressive distances inland from the coast. Even though the origin and dynamics of the Canberra region winds may be more complex, they do share features with other atmospheric flows that may be more directly classified as sea breezes. These include, a diffuse boundary to the circulation and slow inland progress of this boundary during the day, and a more defined rapidly propagating front during the evening [6]. In addition to these features, the over-land and over-ocean components of the sea-breeze circulation are asymmetric [2].

A water tank model was set up to investigate the dynamics of these thermally driven flows. The complete sea/land breeze cycle has been investigated in previous laboratory experiments, see, for example [5]. Other experiments have investigated specific features of the overall flow which are relevant to the present experiments. For example, the leading edge of the sea-breeze flow has been considered to be a gravity current, and the way that gravity current dynamics are modified by ambient turbulence was investigated in [3]. In [8] the circulation driven in a steady symmetrical situation with heating from a horizontal boundary at the bottom of one end of the tank and cooling on the top of the tank at the other end was investigated. The heating and cooling fluxes were only applied over a small fraction of the length of the tank. In a following experiment [9] the overall configuration was similar but the length of the heated region was increased. In this configuration, a front was observed to form between the one-dimensional convective flow over the heated or cooled plate, and the convective flow modified by the circulation between the hot and cold regions. This front was then observed to propagate towards the end of the tank. Another feature of the experiment was that the heating and cooling could be interchanged so that the effect on the flow of a transition to stable forcing could be observed. In the present experiments, the length of the forcing region was extended relative to that in [9] and the forcing was applied asymmetrically, similar to [5]. Thus, the circulation was forced by applying a bottom heat flux to one half of an experimental tank (Figure 1). The heat flux could be rapidly switched between heating and cooling to simulate the diurnal cycle of forcing in the atmospheric boundary layer, while the other, neutral, half of the tank had a constant temperature lower boundary that was maintained approximately midway between the maximum and minimum temperatures for the forced half of the tank.
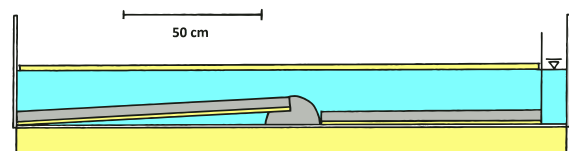

Figure 1: Schematic of the experimental tank. The two heat exchangers are coloured grey, and the insulation is yellow. The tank is shown in the sloping bottom configuration.

The paper begins with a description of the experiment, then moves onto a description of the circulation in the tank and its particular features. It concludes with a brief discussion of the relation of the tank flows to observations in the atmospheric boundary layer.

Experiment

The experiment was carried out in a glass tank, 2 m long by 0.20 m wide. The tank was filled to a maximum depth of 0.15 m. Two aluminium heat exchangers were placed on the bottom of

(a) Particle image over the heated plate

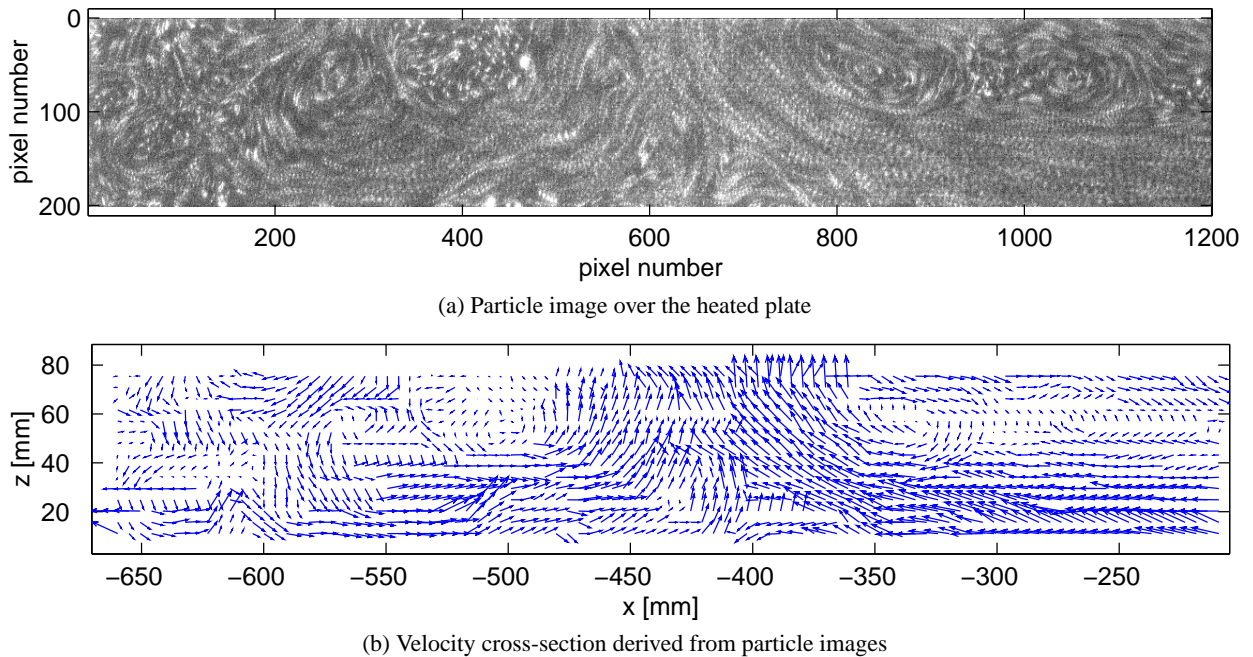(b) Velocity cross-section derived from particle images

Figure 2: (a) Sum of several particle images and (b) velocity cross-section of the thermal front over the heated plate. The origin of the horizontal axis is at the edge of the heated plate, and the lower 0.6 of the water depth is imaged. The experiment was set up with 4° bottom slope. The long axis of the images is parallel to the heat exchanger.

the tank (Figure 1). These could be arranged directly next to each other to form a flat false bottom to the tank, or, as in the figure, alternative unheated sections could be placed between them so that the heated side sloped at either $4.0°$, or $2.2°$ to the horizontal. On the left hand side of the tank, the heat exchanger was connected to hot and cold water circuits with valving such that either circuit could be rapidly switched through the heat exchanger. On the right hand (neutral) side, the heat exchanger was connected to a single circuit with the temperature set to match the initial temperature of the water in the tank. The temperature in all water circuits was controlled by separate thermostatically controlled pump/heater units, and the cooling and neutral side circuits included a refrigerated cooling coil. When water for the warm reservoir was switched through the heat exchanger, there was an initial transient decrease in the temperature in the reservoir; the reservoir temperature then increased linearly with time, so that the system was operating with a constant flux boundary condition. The magnitude of the heat flux was determined by the heating rate that could be supplied by the pump/heater unit. The operation of the cooling cycle was essentially the reverse, with the heat flux being determined by the cooling capacity of the refrigeration unit. The heating and cooling capacity of the system was such that the warm and cool reservoirs returned to close to their set temperatures before the water circuits were switched to reverse the sign of the buoyancy flux.

Vertical sections of the water velocities in sections of the tank were acquired using particle image velocimetry [11, 7]. The water was seeded with size-sorted pliolite particles prior to the start of the experiment. Particle settling in freshwater limited the useful duration of the experiment to two complete heating/cooling cycles (approximately 30 to 35 minutes). A slide projector was used as the light source. Light from the projector was collimated using a 30 cm diameter schlieren mirror and formed into a sheet with cardboard masks. Because of the relatively low light levels, images were acquired with a cooled CCD digital camera. The camera had a high sensitivity and spatial resolution, but its limited data transfer rate restricted the area of the tank that could be imaged. Long images with a small vertical extent (1200 by 200 square pixels) were found to be the most efficient way to use the camera, and, as it turns out, this aspect ratio was quite suitable for recording the flows in the tank.

Temperatures were recorded using four Thermometrics FP10 fast-response thermistors. These were either mounted at fixed locations in the tank and in the warm and cool reservoirs, or mounted on a traversing mechanism so that along-tank temperature profiles could be recorded. When profiling, both temperature and temperature gradients were logged at 100 Hz.

Results

Initial Outflow

When the heating is switched on convection rapidly commences on the heated side of the tank. The horizontal pressure gradient between heated fluid and neutral sides drives an outflow in the form of a gravity current, which propagates into the neutral side fluid along the upper boundary. Buoyancy-inertia scaling [9] suggests that the speed of the gravity current should be $u \sim u_\star$, where $u_\star = (g \alpha F_T h)^{\frac{1}{3}}$ is the convective velocity scale in a layer depth h, heated from below with kinematic flux F_T. g is the acceleration due to gravity and $\alpha = -(1/\rho)(\partial \rho/\partial T)$ is the thermal expansivity. For the present experiment, $u_\star \approx 0.5\,\text{cm}\,\text{s}^{-1}$ and this is consistent with the observed speed of the outflow.

Development of flow over the Heated Plate

In response to the outflow, fluid from the neutral side of the tank begins to move over the heated plate and a circulation is set up. In [9] $u_\star$ scaling, similar to that for the upper outflow from the convective region, was proposed for the speed of the front on the active side. However, as in [9], while the speed of the front between the one-dimensional convective and circulation regimes is constant, it moves approximately 5 times more slowly than the gravity current moving into the neutral side. This reduced

(a) Horizontal temperature profiles, neutral side

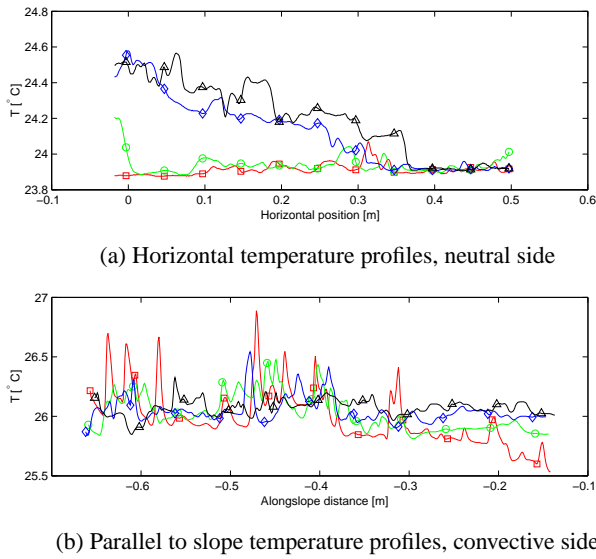(b) Parallel to slope temperature profiles, convective side

Figure 3: Temperature profiles. On the horizontal axis, 0.0 would be the edge of the heated plate. The thermistors were spread evenly in depth with red (squares) closest to the bottom, then green (circles), blue (diamonds) and black (triangles). Temperatures were acquired at 1 mm intervals along the profiles as the thermistors were traversed at $0.1\,\mathrm{m\,s^{-1}}$.

speed could suggest that the flow is no longer governed by an inertia-buoyancy balance; instead the speed of the front may be controlled by a balance between buoyancy and the turbulent stress. This possibility was investigated in [9], but they found it was difficult to find a scaling that could incorporate such a balance and still produce a constant front speed. An alternative interpretation [3] is that the convection is playing an indirect role in the frontal dynamics; the front is still in inertia-buoyancy balance, but the horizontal buoyancy gradient is being reduced by lateral mixing produced by the convection. As a result an internal Froude number, $u/\left(g'h\right)^{\frac{1}{2}}$, with the reduced gravity g' based on the overall density difference across the front, will not represent the actual forcing and will have a smaller than expected value. Particle image and velocity fields, (Figure 2) show that the frontal region is relatively thick ($> 100\,\mathrm{mm}$). Contrast also the sharp change in temperature in Figure 3a at 0.37 m (black trace), corresponding to the thermistor passing into the head of the neutral side gravity current, with the thicker gradient region with superposed warm temperature excursions (thermals) on Figure 3b centred at approximately $-0.38\,\mathrm{m}$, and corresponding to the thermal front visible in the particle image (Figure 2).

The particle image and velocity cross-section (Figure 2) are from an experiment with a $4°$ bottom slope (the images were aligned parallel to the bottom) and show that there is an upslope flow on the left hand side of the thermal front. Thus convergence at the front is driven both by the circulation between the neutral and convective sides of the tank (the "sea-breeze" cell) and the upslope flow on the convective side which is generated by the reduction of the fluid depth (hence faster heating rate) as the front is approached from the left. The along slope temperature gradient on the left hand side of the thermal front is visible in the green temperature trace. That the front is still relatively thick despite the converging flows, reflects the role of the convective turbulence both in driving the mean flows, and mixing the temperature contrasts laterally.

Frontal collapse

Once the left hand heat exchanger is switched to the cooling circuit, the thermal turbulence begins to decay. In Figure 4a, 30 s after the switch, larger vertical velocities are mostly more than 40 mm above the heat exchanger. There is still a remnant of the upslope flow visible, the predominantly along-slope velocity vectors between $-700\,\mathrm{mm}$ and $-500\,\mathrm{mm}$. At the right hand side ($x > -450\,\mathrm{mm}$), the thermal front is visible, with predominantly vertical velocities above 50 mm, and already with a large downslope component between 20 and 50 mm. After 45 s (Figure 4b) the motion driven by convection continues to decay, but the thermal front has both sharpened, and begun to collapse (compare the slope of the front in Figures 4a and b). The rapid sharpening of the front is consistent with the observations of [3] of the rapid formation of a gravity current after the decay of externally driven turbulence.

By 60 s (Figure 4c) the collapsing front resembles a simple gravity current, with a region of recirculation behind the head, (centred at approximately $-470\,\mathrm{mm}$, 70 mm). However, the flow structure is complicated by a thin region of downslope flow that forms ahead of the gravity current and is visible from $-620\,\mathrm{mm}$ to $-670\,\mathrm{mm}$. This flow seems to be a direct result of the buoyancy anomaly created by cooling at the lower boundary, rather than being part of the collapse of the thermal front. The downslope flow intensifies and, after 75 s, extends along the whole lower boundary (Figure 4d). In the next velocity sections in the sequence (not shown), the collapsing flow was being restricted by the end wall, and a return flow was developing above 40 mm height.

Overall, the collapse process has more than a single driving force. In [4] a buoyancy term, due to the temperature anomaly in the flow and the downslope component of gravity, and a thermal wind term, due to the horizontal gradient in the thickness of the cooler fluid, were identified as driving forces of down slope gravity flows. In the flat-bottomed case this second term would be the sole driving force if there was no buoyancy flux at the bottom boundary. However, both are important in the sloping bottom experiment shown and, applying the scaling in [4], should have similar magnitudes. In the present experiments, the cooling at the boundary generates additional buoyancy forcing beyond that generated by the convection and associated circulation. This forcing is not described by the scaling in [4], as its vertical length scale must be related to the transfer of heat out of the fluid due to the cooling. This additional vertical scale is not related to the thickness of the cool layer that is left over from the convective phase of the flow.

Conclusion

Many of the features of the flows observed in these experiments are observed in atmospheric flows. For example, the asymmetry of the over land and over ocean circulations in [2] and the acceleration of the frontal speed in the evening after convection ceases [6]. Similar observations for South-Eastern Australia are in [10]. Wind records for Case II, Figure 9 of [10] show a relatively slow wind change (hence a diffuse front) moving past the observation site in Canberra beginning from approximately 1800 AEDT (Australian Eastern Daylight Time). By the time the change reached Wagga Wagga Airport at approximately 0030 AEDT the following day (Figure 10 of [10]), there was a sharp front with a jump in wind speed to $10\,\mathrm{m\,s^{-1}}$ and simultaneous $90°$ change in wind direction.

Acknowledgements

(a) 30 s

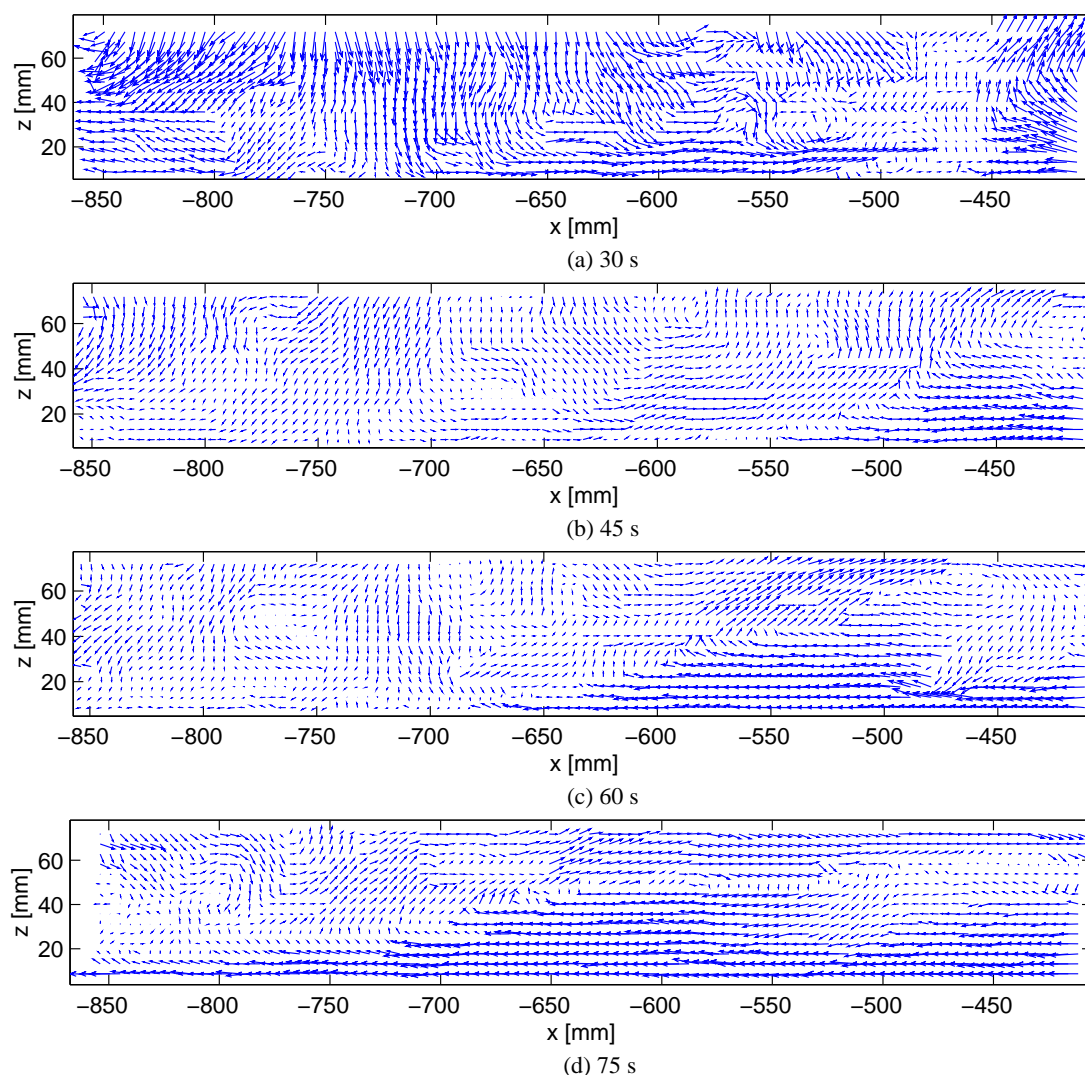(b) 45 s

(c) 60 s

(d) 75 s

Figure 4: Velocity cross sections. Times below the images are the number of seconds after the heat exchanger was switched to the cooling circuit. As for Figure 2, the origin of the horizontal axis is the right-hand edge of the heat exchanger, and the images were acquired parallel to the bottom slope.

References

[1] Clarke, R. H., Fair weather nocturnal inland wind surges and atmospheric bores: Part 1, nocturnal wind surges. *Aust. Met. Mag.*, **31**, 1983, 133–145.

[2] Finkele, K., Hacker, J. M., Kraus, H. and Byron-Scott, R. A. D., A complete sea-breeze circulation cell derived from aircraft observations, *Bound.-Layer Meteor.*, **73**, 1995, 299–317.

[3] Linden, P. F. and Simpson, J.E., Gravity-driven flows in a turbulent fluid, *J. Fluid Mech.*, **172**, 1986, 481–497.

[4] Mahrt, L., Momentum balance of gravity flows, *J. Atmos. Sci.*, **39**, 1982, 2701–2711.

[5] Misumoto, S., Ueda, H. and Ozoe, H., A laboratory experiment on the dynamics of the land and sea breeze, *J. Atmos. Sci.*, **40**, 1983, 1228–1240.

[6] Reible, D. D., Simpson, J. E. and Linden, P. F., The sea breeze and gravity current frontogenesis, *Q. J. R. Meteorol. Soc.*, **119**, 1993, 1–16.

[7] Stevens, C. S. and Coates, M. J., A maximised cross-correlation technique for resolving velocity fields in laboratory experiments, *J. Hydraul. Res.*, **32**, 1994, 195–211.

[8] Sturman, J. J., Ivey, G. N. and Taylor, J. R., Convection in a long box driven by heating and cooling on the horizontal boundaries, *J. Fluid Mech.*, **310**, 1996, 61–87.

[9] Sturman, J. J. and Ivey, G. N., Unsteady convective exchange flows in cavities, *J. Fluid Mech.*, **368**, 1998, 127–153.

[10] Taylor, J. R., Kossmann, M., Low, D. J. and Zawar-Reza, P., Summertime easterly surges in south eastern Australia: a case study of thermally forced flow, *Aust. Met. Mag.*, **54**, 2005, 213–223.

[11] Willert, C. E. and Gharib, M., Digital particle image velocimetry, *Exps. fluids*, **10**, 1991, 181–193.